

Preparation and Properties of Polyamide-6-Based Thermoplastic Laminate Composites by a Novel In-Mold Polymerization Technique

Nadya Dencheva, Ana S. Sampaio, Filipa M. Oliveira, António S. Pouzada, Antonio M. Brito, Zlatan Denchev

I3N—Institute for Polymers and Composites, Department of Polymer Engineering,, University of Minho, Guimarães 4800-058, Portugal
Correspondence to: Z. Denchev (E-mail: denchev@dep.uminho.pt)

ABSTRACT: In this work, a method for preparation of polyamide-6 (PA6) based laminates reinforced by glass fiber- (GFL) or polyamide-66 (PA66) textile structures (PL) via reactive injection molding is disclosed. It is based on in-mold anionic polymerization of ϵ -caprolactam carried out at 165°C in the presence of the respective reinforcements performed in newly developed prototype equipment whose design concept and operation are described. Both composite types were produced for reaction times of 20 min, with conversion degrees of 97–99%. Initial mechanical tests in tension of GFL samples displayed almost twofold increase of the Young's modulus and stress at break values when compared with the neat anionic PA6. The improvement was proportional to the volume fraction V_f of glass fiber fabric that was varied in the 0.16–0.25 range. A 300% growth of the impact strength was registered in PL composites with V_f of PA66 textile of 0.1. Removing the surface finish of the latter was found to be a factor for improving the adhesion at the matrix–fiber interface. The mechanical behavior of GFL and PL composites was discussed in conjunction with the morphology of the samples studied by optical and electron microscopy and the matrix crystalline structure as revealed by synchrotron X-ray diffraction. © 2013 Wiley Periodicals, Inc. *J. Appl. Polym. Sci.* **2014**, *131*, 40083.

KEYWORDS: polyamides; thermoplastics; synthesis and processing; ring-opening polymerization; composites

Received 15 August 2013; accepted 20 October 2013

DOI: 10.1002/app.40083

INTRODUCTION

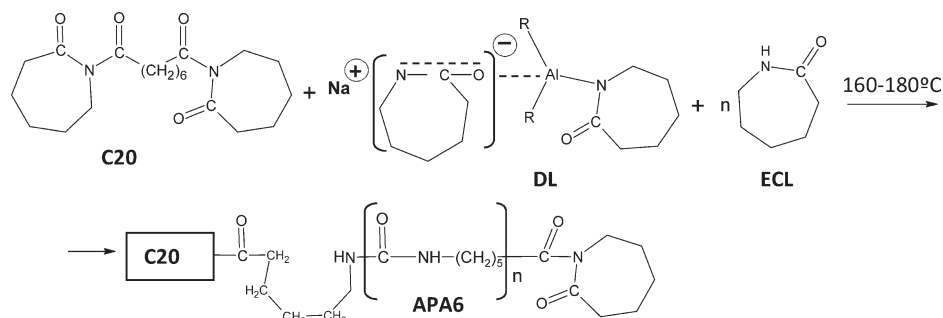
Polymer composites with thermoplastic matrices (TPCs) comprising particulate or fibrous reinforcements are being used in steadily increasing number of diverse fields because of their good material performance and manufacturing flexibility.¹ TPCs offer some important advantages over their thermoset counterparts, such as higher toughness of the matrix, higher impact resistance, and significantly shorter manufacturing cycles. In addition, these composites are of light weight, can be welded,² and relatively easily recycled by reprocessing.³ The latter feature becomes very important in view of the rigorous requirements for environmental protection imposed in most industrialized countries.

TPCs may be produced by either melt-processing or reactive processing. The melt-processing techniques require melting of already existing thermoplastic material in the presence of the reinforcing component—particulate, fibrous, or layered. Because of the high melt viscosity of the polymer matrix, elevated processing temperatures and pressures have to be applied to impregnate the reinforcements. Nevertheless, proper impregnation at a microscale in fiber-reinforced TPCs is not easy. Quite often, materials with significant void content are produced that lead to insufficient mechanical properties.⁴ In the case of TPCs with

particulate and layered inorganic reinforcements, melt-processing can result in poor dispersion of the reinforcing component and/or agglomeration with similar negative influence on the mechanical properties.⁵

Various strategies are developed in the melt-processed TPCs to avoid the above problems. In fiber-reinforced systems, matrix material and reinforcements are often combined prior to the manufacturing of the finished article by prepregging,⁶ film stacking,⁷ preparation of powder-impregnated, comingled,^{8,9} or braided hybrid yarns.¹⁰ The final part is prepared by different consolidation techniques including compression molding, pultrusion, autoclave processing, or tape placement.¹¹ The common shortcoming of these approaches is the elevated costs of both raw materials and manufacturing rendering them feasible for high-performance applications only. Moreover, melt-processing of TPCs requires several heating–cooling cycles, whereby some thermoplastics with relatively high melting points, for example, polyamides and aromatic polyesters, can undergo slight to moderate degradation to the detriment of their mechanical properties.

A key for the cost-effective preparation of homogeneous TPCs with optimum impregnation of the reinforcements by the matrix material can be the significant decrease of the viscosity



Scheme 1. Schematics of the chemical reactions and catalytic system components in AAROP: C20, Bruggolen C20 (activator); DL, dicaprolactamato-bis-(2-methoxyethoxy)-aluminate; R = OCH₂CH₂OCH₃ (initiator); ECL, ϵ -caprolactam; and APA6, anionic polyamide-6. The structure of DL is according to that given in Ref. 26. The structure of C20 is based on the current analyses.

of the latter. This is possible in the reactive processing techniques, where the TPC is obtained *in situ*, through polymerization of low-viscosity monomers or oligomers in the presence of the reinforcements. The respective monomer has to produce high-molecular-weight linear polymer formed at sufficiently high conversions, without generation of byproducts.

Among the polymerization types meeting these requirements, the most common is the ring-opening polymerization (ROP).¹² It is based on anionic or cationic reaction mechanisms, in which ring-shaped monomer molecules are opened and transformed into high-molecular-weight polymers. Thus, polyamide-6 (PA6) can be produced through activated anionic ROP (AAROP) of the inexpensive ϵ -caprolactam (ECL). The viscosity of the molten ECL at 110°C is in the range of 50 MPa,¹³ which is more than 10 times lower than that of PA6 at 250°C and similar share rate. The process is carried in a way that the ECL polymerization and PA6 crystallization occur simultaneously at temperatures with 40–60°C lower than the melting point of the resulting anionic PA6 (APA6). The AAROP of lactams to neat polyamides is thoroughly documented¹⁴ and well understood. Strong bases such as metal caprolactamates are most often used as initiators of the process and imide group-containing compounds (e.g., acyl lactams) as activators, which help to overcome the induction period so that the polymerization process is completed after several minutes.¹⁵ This radically reduces the overall production cycle time and increases the energy efficiency of the process.

Numerous studies exist on reactive processing toward APA6 materials, but only a few of them deal with the preparation of composites. Processes related to resin transfer molding (RTM), reactive injection pultrusion (RIP), reactive vacuum infusion (RVI), and reactive rotational molding (RRM) are most frequently used. Thus, Gong and Yang¹⁶ produced all-polyamide TPCs by RTM in which the PA6 matrix was formed by in-mold AAROP of ECL in the presence of unspecified amount of polyamide-66 (PA66) plain cloth. With the polymerization temperature range being between 160 and 180°C, void fractions of 1.0–1.2% were found. Luisier et al.¹⁷ developed a pilot RIP line for the *in situ* AAROP of lauryllactam to polyamide-12-based, glass fiber-reinforced TPCs. Modeling of all phenomena involved was presented aiming to the development of optimization strategies and engineering tools to control the process. Earlier study reported on a similar RIP process for the preparation

of fiber-reinforced APA6.¹⁸ A series of articles disclosing RVI for manufacturing of PA6 glass fiber composites have demonstrated the potential of this technique for industrial application.^{19,20} Harkin-Jones and Crawford^{21,22} explored for the first time the RRM of liquid plastic feedstock comprising a mixture of activated ECL and nylon prepolymer. Neat APA6 and TPCs with glass fibers were prepared and tested with good results. Recently, this technique was revisited using only activated and initiated ECL for the preparation of neat APA6.²³

It can be concluded that the studies on reactive processing of APA6-based composites attract a constant interest rendering a variety of processing techniques. This work describes the use of recently developed prototype semiautomatic equipment for reaction injection molding of nylons (NY-RIM) to prepare APA6 thermoplastic laminates by *in situ* AAROP of ECL in the presence of glass and polymer fabrics. The RIM concept is widely used for the production of polyurethane-based finished parts^{24,25}; however, to the best of our knowledge, no studies exist on its application to polyamide laminate composites. This work describes the principle of the NYRIM technology (semiautomatic prototype equipment for polyamide RIM), which is mixing of two monomer feeds by jet impingement and the subsequent automatic transfer of the activated and initiated ECL into a preheated mold that contains the reinforcements—glass fiber or PA66 textile structures. The AAROP is carried out in the mold to get the final TPC laminates comprising the *in situ* prepared APA6 matrix and the respective reinforcement. Some initial studies on the mechanical properties of the resulting TPCs in tension and impact are reported. Morphological studies by light and electron microscopy are also presented. Initial X-ray diffraction studies of the APA6 matrix are performed to trace the influence of the reinforcement on its crystalline structure.

EXPERIMENTAL

Materials

ECL monomer with reduced moisture content suitable for AAROP (AP-Nylon® caprolactam) was delivered from Brüggermann Chemical, Germany. It was kept under vacuum for 1 h at 23°C before use. Bruggolen C20® (C20) of the same manufacturer was used as polymerization activator. It contains up to 17% of active isocyanate groups. The supposed chemical structure of C20 is presented in Scheme 1. The

initiator sodium dicaprolactamato-bis-(2-methoxyethoxy)-aluminate [Dilactamate® (DL); Scheme 1] was purchased from Katchem, Czech Republic, and used without any further treatment.

The glass fiber reinforcements were supplied by PPG Industries Fiber Glass. Three fabric types of plain-weave E-glass were used with areal densities of 210, 300, and 482 g/m² treated with proprietary sizing suitable for polyamide laminates.

The PA66 reinforcement fabric is typically used in automotive airbags (plain weave, silicone coated, 525 denier/580 dtex, 43 × 44, areal density 110 g/m²) commercialized by Autoliv, Sweden. In some cases, these fabrics were treated with acetone for 30 min and dried at room temperature before use to remove the silicone coat.

Preparation of Composites

The ECL monomer is separated into two equal portions and placed into two heated flasks with magnetic stirrers. To the first of them, 1.5 mmol of DL is added, and to the second, 0.75 mmol of C20 is added whereby maintaining the temperature in the 90–110°C range. The in-mold AAROP is performed in the NYRIM equipment the concept of which is schematically shown in Figure 1.

The production cycle starts with introducing the ECL/C20 and ECL/DL feeds separately through the two inlets [Figure 1(B), position 3] into the mixing camera (position 1) preheated to 110°C. By simultaneous actuation of the hydraulic cylinders C2 and C3, the two material batches are mixed by jet impingement. Right after that C1 introduces the initiated and activated ECL into the previously closed mold (position 2) preheated to the polymerization temperature and already containing the respective amount of the glass fiber textile or PA66 textile reinforcements. After elapsing the preset time for AAROP, the mold cools down automatically to a preset temperature of about 60°C and opens through C4, thereby ejecting the molded composite plate (80 mm × 80 mm × 3 mm). Figure 2 shows the configuration of the opened mold with the fabrics inside and the geometry of the molded composite plates. In this study, the AAROP is performed at 165°C, setting the reaction time at 20 min. These conditions were found to be optimal in earlier studies using the prototype NYRIM equipment.²⁷

Samples of hydrolytic PA6 (HPA6) were produced by compression molding at 240°C, and 5 MPa of a medium-viscosity, general purpose commercial-grade PA6 (Durethan B30S, Lanxess). They were used for comparison in the mechanical and structural tests of this study.

The description and designations of the laminate composites prepared by AAROP in the NYRIM mold in the presence of the respective glass fiber or PA66 textile reinforcements are summarized in Table I. The respective percentage of reinforcing textile in laminates reinforced by glass fiber (GFL) and APA6-based laminates reinforced by PA66 (PL) composites was calculated on the basis of the effective volume of the quadratic mold and the weight of the monomer necessary to fill it considering a small excess to compensate the volume contraction after polymerization. The following amounts of layers were necessary in

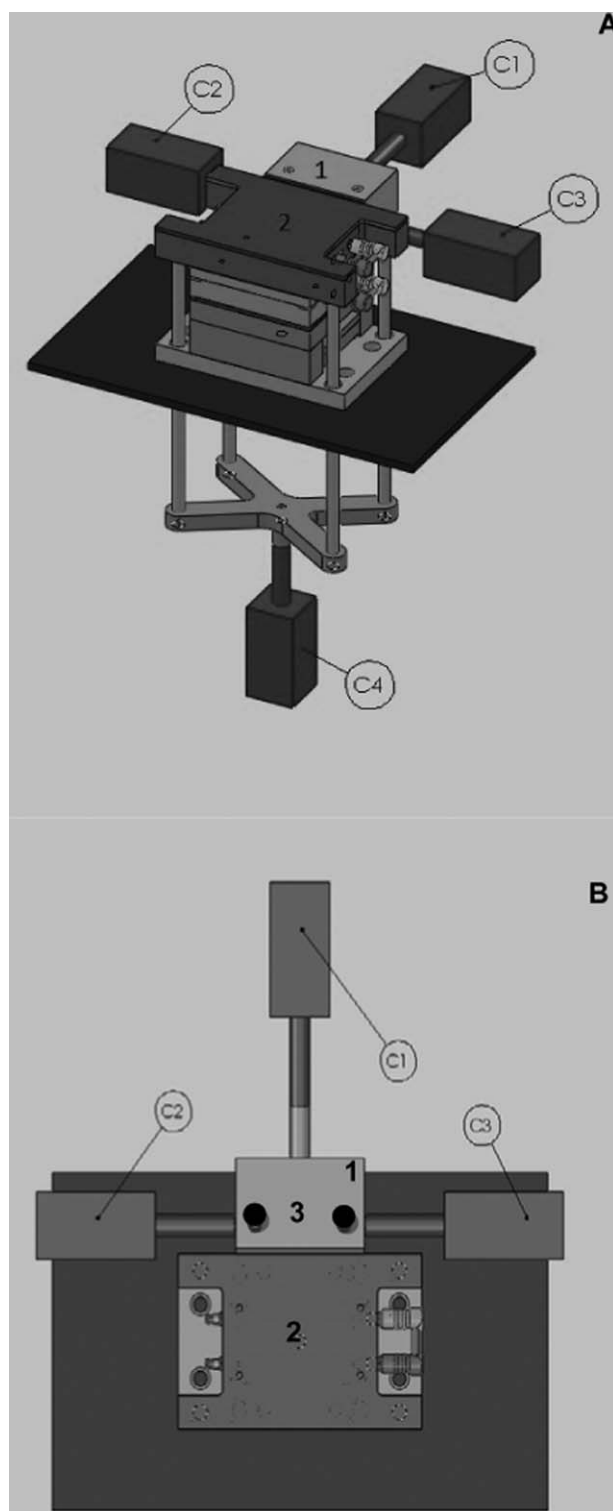


Figure 1. Prototype NYRIM processing machine concept: (A) side view and (B) top view; 1: preheated camera for mixing by jet impingement; 2: the top plate of the mold; 3: inlets for the two material feeds of the premixing camera; and C1–C4: hydraulic cylinders.

the GFL composites to adjust the textile reinforcement weight to 20 wt %: GFL1, six layers; GFL2, five layers; and GFL3, three layers. In the case of PL, three to four layers were needed. To

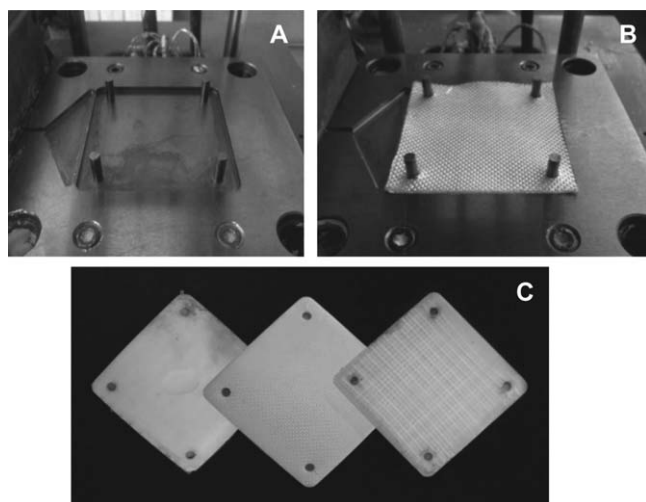


Figure 2. A: Configuration of the opened mold. B: The mold with the fabrics of the reinforcement. C: Finished laminate plates.

calculate the volume fraction V_f of the textile reinforcement knowing the laminate thickness t , the aerial density A_w , the number of plies n , and the density of the reinforcement ρ_f the following relation was used²⁸:

$$V_f = \frac{n \times A_w}{\rho_f \times t}$$

The APA6 sample represents neat matrix material prepared via AAROP in the NYRIM mold at the same processing conditions as the laminate composites.

Table I. Sample Description and Designation

Sample description	Reinforcement amount (wt %) and type	Volume fraction ^a	Sample designation
Neat hydrolytic PA6	-	-	HPA6
Neat anionic PA6	-	-	APA6
Glass fiber/APA6 laminates	20; low density ^b	0.16	GFL-1
	20; medium density	0.19	GFL-2
	20; high density	0.27	GFL-3
PA66 fabrics/APA6 laminates	10	0.09	PL-10
	10; pretreatment ^c	0.09	PL-10A
	15	0.13	PL-15
	15; pretreatment	0.13	PL-15A

^aThe volume fraction of the reinforcements was calculated according to Ref. 28.

^bGlass fiber textile structures with area densities: low: 210 g/m²; medium: 300 g/m²; and high: 482 g/m². The areal density of the PA66 fabric is 110 g/m².

^cImmersion in acetone at 23°C for 30 min followed by drying at 23°C.

Characterization of Composites

The degree of AAROP conversion was determined as a relationship of the mass of the sample after and before Soxhlet extraction with methanol during 8 h until constant weight. Values in the range of 97–99% were reached. In all composites, no inhibition of the polymerization process was observed. The composites were then subjected to a series of mechanical and structural tests.

The tensile tests were performed with an Instron model 4505 tensile testing machine. The tests were carried out at 23°C ± 2°C with a standard load cell of 50 kN at a constant crosshead speed of 50 mm/min. From the different composite plates prepared in the NYRIM machine, standard specimens for tensile tests according to DIN 53504-S3 were cut out with overall length 35 mm and sample thickness of 3.0 mm, and the distance between the grips being 25 mm. At least five specimens of each sample were studied to calculate the average and standard deviation data. The engineering stress was determined as the ratio of the tensile force to the initial cross section of the sample. The engineering strain was determined as the ratio of the sample gauge length at any time during drawing to that before drawing. The stiffness was calculated as the secant modulus from the stress–strain curves at 1% strain. In all cases, samples conditioned for about 30 days at 23°C and 65% relative humidity were tested.

The study of the impact resistance of the composite materials was done by means of Charpy impact test according to ISO 179. Standard test bars were cut out of the molded plates with dimensions of 80 mm × 10 mm × 3 mm that were notched with radius of curvature of 0.25 mm to a depth of 2.54 mm. The notched impact strength was calculated as the impact energy absorbed relative to the test bar cross section. At least 5 bars from every composite were tested to determine the standard deviation data.

The wide-angle X-ray scattering patterns (WAXS) in this study were registered at the Soft Condensed Matter Beamline (A2) of HASYLAB, Hamburg, Germany, using synchrotron radiation with a wavelength fixed to 0.15 nm. The sample-to-detector distance was set at 90 mm, with the diffraction patterns being registered by means of a MARCCD two-dimensional detector of Rayonix. The samples were studied in transmission mode with an exposure time of 25 s. A specially designed sample holder was used allowing for controlled heating–cooling cycles in the 30–300°C range. An Imago multichannel processor and program controller of JUMO GmbH were used to regulate the sample temperature in heating and cooling. The difference between the read-out and real temperature was found to be 3–4°C at the heating rate of 20°C/min applied in this study. Corrections for background scattering, irradiated volume, and beam intensity were performed for each 2D pattern. For further data processing, a commercial software package was used. Peak-fitting was applied in the linear WAXS patterns obtained after integration in the range between scattering angles 2θ of 3° to 40°.

The scanning electron microscopic (SEM) analysis was performed in a NanoSEM-200 apparatus of FEI Nova. The samples were prepared by cryogenic fracture after immersion in liquid

nitrogen. For the transmission light microscopy (LM) study, an Olympus BH-2 microscope was used, and the composite samples were prepared by microtoming.

RESULTS AND DISCUSSION

The chemistry of the AAROP of ECL is well known since the early 1970s. Scheme 1 gives an idea of the accepted reaction mechanism.¹⁴ Thus, AAROP in this work is initiated by the basic DL—an organoaluminum compound that contains a stabilized caprolactamate anion.²⁹ The activator C20 contains two preformed imide links $C(O)-N-C(O)$, in the presence of which polymerization starts directly with the propagation reaction. The AAROP conditions, for example, composition of the catalytic system, reaction temperature, time duration of the NYRIM process, and cooling conditions, were optimized in previous studies toward the production of high-molecular-weight APA6 matrix with $M_n > 35,000$ with an ECL conversion of 97–99%.^{26,27}

Mechanical Properties of the Composites

Figure 3 shows representative stress–strain curves of the APA6-based laminate composites of this study and of the neat APA6 matrix obtained by the NYRIM process at 165°C. As expected, the curve of the neat matrix material displays clear elastic and plastic regions. Very similar stress–strain curves were obtained previously with compression-molded isotropic plates of neat HPA6 annealed at 160°C.³⁰ The incorporation of 20 wt % glass fiber reinforcement results in a complete disappearance of the plastic deformation plateau in the GFL composites. In addition, significant growth of the stress at break (σ_{br}) and steeper slopes of the Hookean region of the curves are also observed, whereby the higher the density of the glass fiber fabrics, the stronger and stiffer are the TPCs.

The tensile behavior of the PA66-reinforced laminates is quite different. As seen in Figure 3, instead of yielding, a well-expressed strain-hardening process starting at deformations above 5% is observed. The relatively short elastic regions are with reduced slopes. The curves also indicate the growth of the tensile strength when the amount of PA66 textile reinforcement

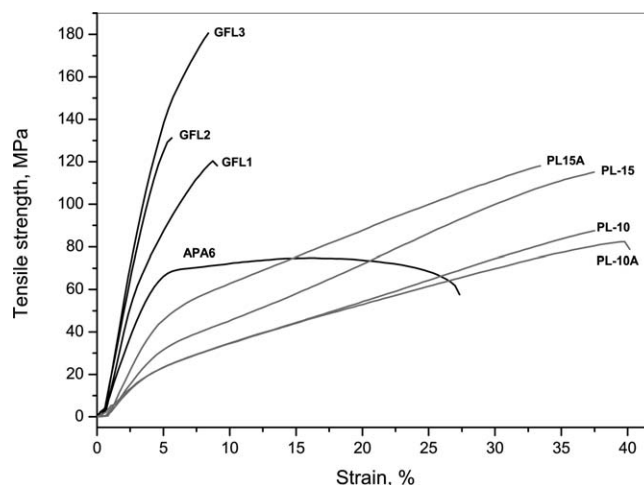


Figure 3. Representative stress–strain curves in tensile mode of laminate composites comprising APA6 matrices reinforced by glass fiber (GFL) or PA66 (PL) fabrics. For sample designations, see Table I.

increases from 10 to 15 wt %. The elimination by the acetone treatment of the silicone sizing of the textile structures improves the mechanical performance only in the sample with 15 wt % of reinforcement.

Table II includes the numerical data extracted from the stress–strain curves in Figure 3. Previously obtained data for HPA6 compression molded from granules and annealed at 160°C are also included for comparison. In comparison with HPA6, the anionically produced neat matrix APA6 has lower deformation at break, higher E , and σ_{br} , with the improvement factor IF being of 60% and 40%, respectively. Provided that all samples of this study are mechanically tested after prolonged storing at 23°C and 65% relative humidity, they are expected to be conditioned. This explains why the E -values for neat HPA6 and APA6 are relatively low, that is, in the range of 1.0–1.6 GPa. Testing of conditioned samples was accepted as it has a better relationship with the long-term exploitation of polyamides. The E -values for dried samples can be twice as high but rapidly deteriorate at environmental exposure.

Table II. Mechanical Properties in Tensile Mode (DIN 53504-S3) of Glass Fiber and PA66 Fabrics-Reinforced APA6 Laminates

Sample designation	Young's modulus (E) (GPa)	IF ^a (%)	Stress at break (σ_{br}) (MPa)	IF ^a (%)	Strain at break (ϵ_{br}) (%)
HPA6	1.0 ± 0.1	–	47 ± 2	–	70 ± 18
APA6	1.6 ± 0.2	60/0	66 ± 2	40/0	11 ± 3
GFL-1	3.0 ± 0.1	200/88	123 ± 5	162/86	6 ± 1
GFL-2	3.2 ± 0.2	220/100	131 ± 4	178/99	5 ± 1
GFL-3	4.1 ± 0.1	310/175	185 ± 9	294/180	7 ± 1
PL-10	0.8 ± 0.1	–20/–50	82 ± 5	75/24	39 ± 3
PL-10A	1.0 ± 0.2	0/–38	70 ± 8	49/6	42 ± 4
PL-15	0.9 ± 0.1	–10/–44	93 ± 7	98/41	32 ± 5
PL-15A	1.3 ± 0.3	30/–19	94 ± 7	100/60	32 ± 3

^aIF, improvement factor. $IF = \frac{A_{TPC} - A_{matrix}}{A_{matrix}} \times 100\%$, wherein A_{TPC} is the value of E or σ_{br} of the respective thermoplastic composite and A_{matrix} of the respective neat matrix. For each composite, IF is calculated with respect to both HPA6 (first value) and APA6 matrices. In all cases, samples conditioned for about 30 days at 23°C and 65% relative humidity were tested.

Table III. Charpy Impact Strength (DIN EN ISO 179) of Selected TPC Samples

Sample designation	Impact strength (kJ/m ²)	IF (%) ^a
HPA6	7–15 ^b	–
APA6	68 ± 7	0
GFL-1	143 ± 10	110
GFL-2	158 ± 9	132
GFL-3	201 ± 11	196
PL-10A	295 ± 14	334

^a IF was calculated with respect to the APA6 matrix.

^b Neat PA6 (Akulon K224) of DSM, The Netherlands (manufacturer's data sheets).

The tensile properties of the GFL composites with volume fractions V_f of reinforcements in the 0.16–0.25 range were several times superior in comparison with either neat APA6 or HPA6. As expected, the GFL-3 composite with the densest glass fiber fabrics, that is, with the highest V_f , displayed the highest modulus value of above 4 GPa and stress at break of 185 MPa, maintaining the deformation at break in the 5–7% range.

The PA66-reinforced laminates have different mechanical properties in tension. Thus, in all PL composite in Table II, the moduli are lower than those of the neat APA6 and close to HPA6. At the same time, ε_{br} grows to 32–42% and σ_{br} continues to be significantly better than APA6 or PA6 with values in the range of 80–90 MPa corresponding to IF values between 50 and 100%. Evidently, by changing the amount and type of the reinforcing fabric material and its sizing, one can control in a wide range the stiffness and strength of the APA6 laminate composites, as well as their overall response to external loading.

The question arises whether the E -values of GFL and PL samples in Table III correspond to the theoretical data calculated according to the “Law of Mixtures” frequently used for micro-mechanical characterization of composite samples. It should be noted that the plain-weave fabrics of glass or PA66 fibers should be considered quasi isotropic reinforcement for which the following relation was suggested³¹:

$$E_{\text{comp}} = \frac{3}{8} \alpha_f E_f + \frac{5}{8} \alpha_p E_p,$$

where E_{comp} is the theoretical values of the composite's Young's modulus, α_f and E_f are the volume fraction and Young's modulus of the fiber reinforcement, respectively, and α_p and E_p are the respective values of the matrix material. E_f values of 70 GPa (E-glass) and 1.5 GPa (conditioned PA66) were assumed. The E_p value of neat APA6 of 1.6 GPa was determined in this study. The use of the above equation renders theoretical E -values of 3.5 GPa for GFL composites and 0.94–0.96 GPa for the PL composites, that is, a full agreement with the real values of the respective samples in Table III is observed.

The initial Charpy impact tests with selected TPC samples are shown in Table III. Impact strengths were obtained with

improvement factors with respect to the neat APA6 from >110 to >300%, which shows the good potential for industrial application of the glass- and PA66-reinforced APA6 laminates obtained in the NYRIM equipment.

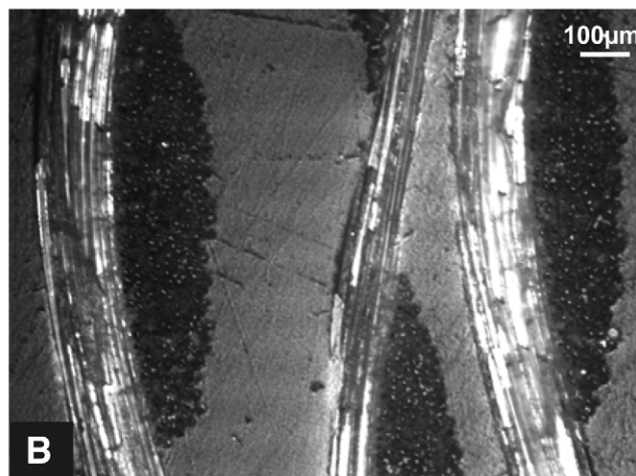
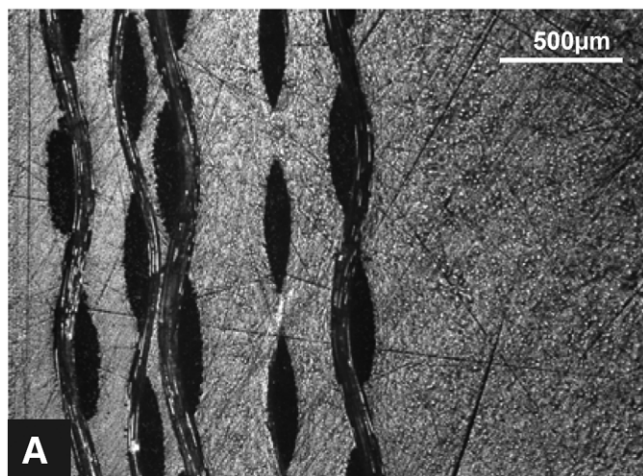
Microscopy Studies

The morphology of the laminate composites in this study was characterized by LM and/or SEM. All GFL materials and the PA66-reinforced APA6 laminates, in which the textile fabrics were subjected to acetone treatment, were impossible to fracture even after prolonged immersion in liquid N₂, and thus, it turned to be impossible to study them by SEM. The GFL samples were successfully microtomed and observed by LM in reflection mode (Figure 4). This technique, however, did not produce images with sufficient quality for the PL-10A and PL-15A samples. The PL-10 and PL-15 composites were the only ones that cryofractured, which enabled the SEM morphological studies (Figure 5).

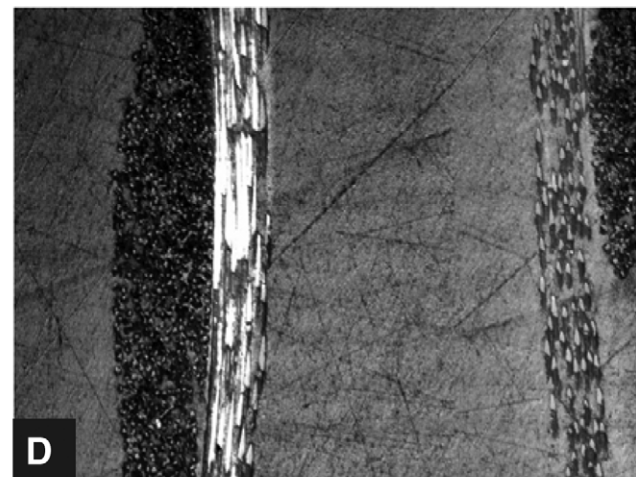
Figure 4 shows the relatively homogeneous distribution of the three glass fiber reinforcements with fiber diameters of 20–25 μm in the APA6 matrix. Although the configuration of the textile structures in GFL-1 and GFL-2 seems quite similar [Figure 4(A,C)], GFL-3 [Figure 4(E)] shows different weave structures, the predominant orientation of the single glass fibers being parallel to the plate surface and normal to the microtoming direction. In addition, the reinforcing fabrics in GFL-3 sample are made of thicker fibers, as seen from the image in Figure 4(F). Good impregnation of the fibers is observed in all GFL samples with no indications for the presence of voids.

The morphology of the PL-10 and PL-15 laminate composites can be observed in Figure 5 with SEM images allowing for observation of the matrix–fiber interface and the morphology of the PA66 fibers themselves. From Figure 5(A) it becomes evident that in the laminate with 10 wt % of PA66 reinforcements, the APA6 matrix material seems to have entered between the fibers of the textile structure and wetted them well. At higher magnification of the next images, it is possible to observe the PA66 fiber–APA6 matrix interface in the PL-10 sample, proving the existence of some cracks and voids [Figure 5(B)] and of many fine crosslinks between the matrix and fibers [Figure 5(C)], to which the good impact resistance of the PA66 laminate composites should be attributed. Increasing the reinforcement percentage to 15% resulted in poorer penetration of matrix material between the textile fibers, leaving on them some “dry” areas, especially in the bulk of the sample [Figure 5(D)]. Figure 5(E) image shows a close-up of a bundle of PA66 fibers whose average diameter is 26 μm , with smooth surface and an apparent shell–core structure. Figure 5(f) shows the good interaction at the fiber–matrix interface for this sample, which again should be related to the good tensile and especially impact properties of the PA66/APA6 laminates. The impossibility to fracture the PL-10A and PL-15A samples is an indirect proof that removing the silicone sizing by acetone treatment leads to stronger interaction between the matrix and the textile fabric. This is to be expected considering the chemical similarity of PA6 and PA66 and the capacity of their amide groups to participate in H-bond formation and even chemical interactions across the interface.

GFL-1



GFL-2



GFL-3

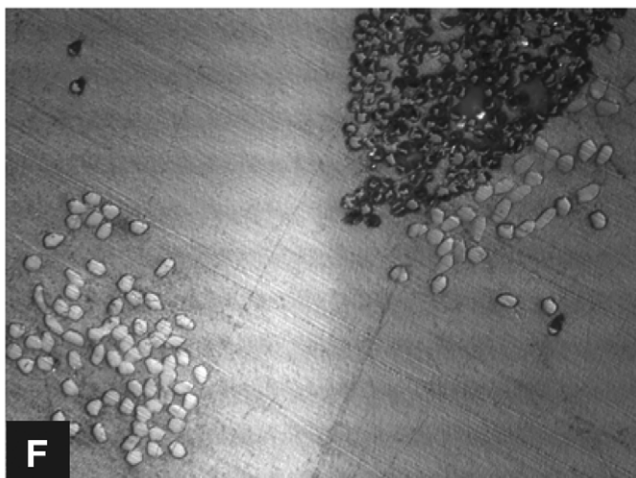


Figure 4. Reflection light microscopy images of APA6/glass fiber composites obtained at magnifications of $\times 5$ (A, C, and E) and $\times 20$ (B, D, and F). Composite designations are according to Table I. Each laminate contains five layers of glass fiber fabrics with different densities and weave types corresponding to 20 wt % with respect to ECL.

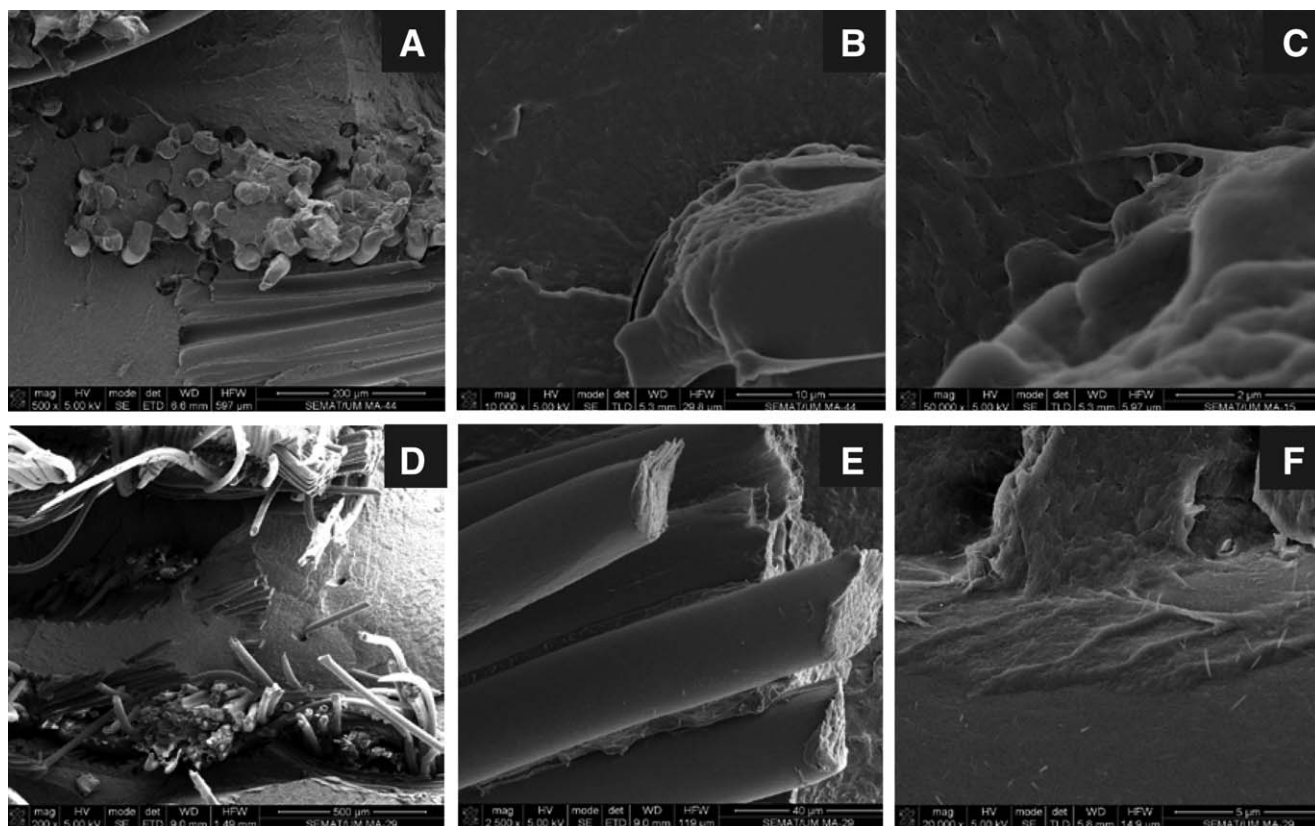


Figure 5. SEM images with various magnifications of APA6/PL laminate composites comprising 10 wt % (A–C) and 15 wt % (D–F) of PA66 reinforcing fabrics without treatment with acetone.

WAXS Structural Studies

PA6 is a semicrystalline polymer characterized by two basic crystalline modifications, α - and γ -polymorphs, that normally coexist. Which one of them is predominant will depend on the temperature of crystallization, externally applied forces, and the presence of moisture or of certain additives.³² Thus, slow cooling after melting of PA6 leads to predominance of the α -polymorph, whereas the γ -polymorph is formed when external force is applied. The α -polymorph is monoclinic, characterized by two WAXS reflections with 2θ angular positions at about 19° and 23° . The pseudo-hexagonal γ -form exhibits one or two very close reflections at about 21° .³³ It was established by many authors that the polymorph content of PA6 and the α/γ relationship were directly related to its mechanical behavior (Ref. 26 and references therein).

To study the influence of the type and amount of the textile reinforcement on the crystalline structure of the APA6 matrix, synchrotron WAXS studies were performed with the GFL and PL samples. Figure 6 displays the WAXS patterns of the as-prepared GFLs at 30°C [Figure 6(A)] and after melting of the matrix and its recrystallization [Figure 6(B)]. Table IV summarizes the data on degree of crystallinity and polymorph content of all glass fiber laminates obtained from the WAXS patterns in Figure 6 through a fitting procedure described elsewhere.³⁰ In all the as-prepared GFL materials, as well as in the neat APA6 matrix obtained under the same NYRIM

conditions, the overall crystallinity index changes in the 46–49% range (Table IV), the variation being comparable with the accuracy of the measurement. The compression-molded neat HPA6 (presented to enable comparison) shows the lowest crystallinity of 43% and the highest α -PA6 content, which can be attributed to the compression-molding process using pressure.^{26,32}

In the as-prepared GFL samples, the α/γ ratio displays little sensitivity to the presence and type of glass fiber reinforcements, being in the range of the experimental error. Hence, it may be supposed that the type of the glass fiber fabric do not influence the PA6 polymorph content in the as-prepared samples. It should be noted that during the *in situ* AAROP in the NYRIM mold, two simultaneous processes occur. First, a polymerization process takes place, in which the macromolecules of the APA6 matrix are produced. Second, a crystallization process also occurs because the NYRIM processing is carried out far below the melting point of the *in situ* formed APA6 matrix. The fact that the presence of glass fibers in the as-prepared GFL does not result in significant changes in α/γ values means that no steric hindrance effects are present in this case, and thus the just formed PA6 macromolecules when crystallizing can assume the conformation necessary for the formation of the α -polymorph. If the GFL is subjected to melting/recrystallization (Table IV, Column 2), the variations of the α/γ ratio become statistically significant showing an increase of the γ -PA6 proportional to the fabrics density, that

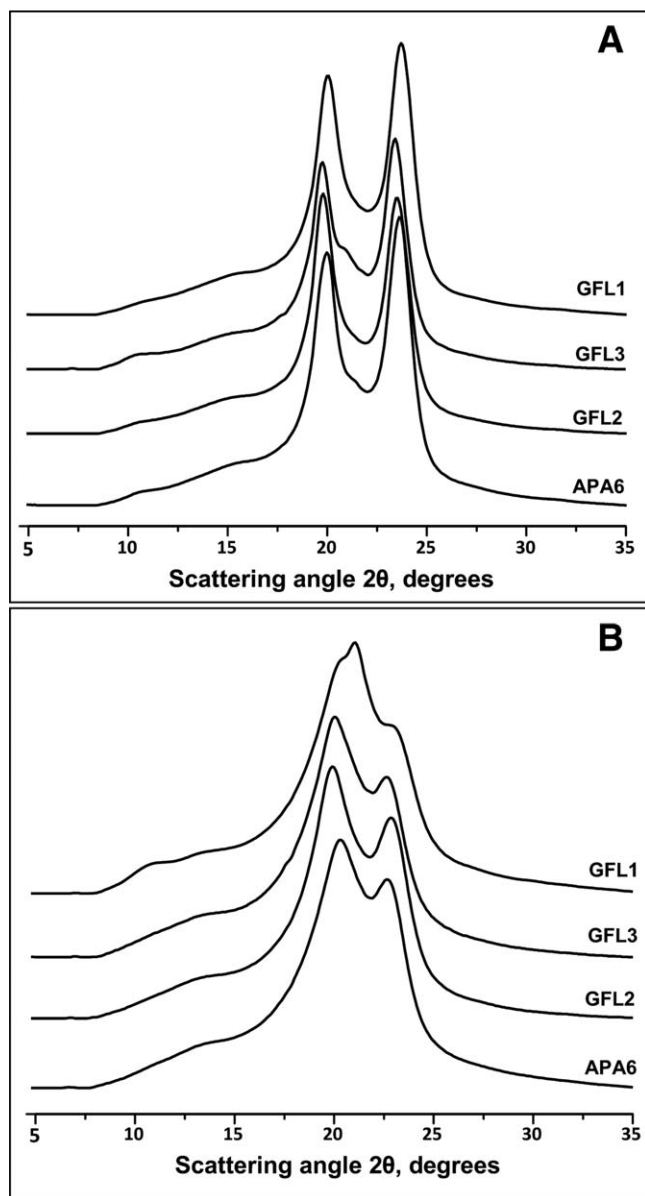


Figure 6. WAXS patterns of APA6/GFL of (A) as-prepared composites and (B) after melting at 260°C and recrystallization of the matrix.

is, V_f . This observation may be used for optimization of the mechanical properties of GFL by their thermal annealing, having in mind that the polymorph content in PA6-based materials has a direct influence on their mechanical properties.^{30,33}

A comparison of the WAXS profiles of the same sample set after melting the matrix APA6 at 260°C and its nonisothermal recrystallization is shown in Figure 6(B). This heat treatment was performed while irradiating the samples in the synchrotron beamline. Under these conditions, crystallization of already existing PA6 macromolecules only takes place. Although in the neat APA6, the amount of α -PA6 almost doubles, in the GFL materials, there is an increase of the γ -PA6 content proportional to the density of the glass fiber fabric (Table IV) changing the α/γ ratio from 3.97 (APA6) to 2.91–0.62 (GFL1–GFL3).

Table IV. Overall Crystallinity and Polymorph Content in Laminate Composites Comprising 20 wt % of Glass Fiber Fabrics with Various Densities When Compared with That of the Respective Neat Matrix

Sample	As prepared		After recrystallization	
	Crystallinity (%)	α/γ	Crystallinity (%)	α/γ
HPA6	42.6	1.43	41.6	9.68
APA6	45.8	1.84	47.7	3.97
GFL1	47.6	1.56	45.4	2.91
GFL2	46.8	1.08	45.3	1.85
GFL3	48.8	1.61	48.9	0.62

Apparently, whenever the already existing PA6 phase crystallizes from the melt in the presence of glass fiber reinforcements, the γ -type nucleation becomes predominant, increasing in the order from GFL1 to GFL3, thus favoring the formation of γ -PA6 polymorph. Therefore, the closer the contact of the recrystallizing PA6 with the E-glass fiber, the larger becomes the amount of the γ -PA6 polymorph. Such trend was repeatedly registered in other PA6 composite systems obtained by melt-mixing, for example, in montmorillonite-reinforced PA6 composites.^{34,35}

The effect of the PA66 textile reinforcement on the degree of crystallinity and the polymorph content of the APA6 matrix was also studied by WAXS changing the temperature in the 30–260°C range. Figure 7(A,B) represents the WAXS profiles of the laminate composites containing 10 wt % of PA66 fabrics without and with acetone treatment, respectively. In the latter case, the PA66 fibers can directly influence the crystallization of the adjacent APA6 matrix material. Analyzing all WAXS profiles allows the conclusion that the presence of reinforcements does not hinder the Brill transition characteristic for PA6. Thus, increasing the heating temperature from 30 to 200°C (Curves 2–4 in both subfigures) leads to a pronounced α -to- γ -phase transition.

Table V includes the overall crystallinity indices and the α/γ values in the APA6 matrix computed by deconvolution of some of the WAXS profiles in Figure 7. It should be noted that a nonisothermal polymerization process was applied here that was found to be optimal for the ECL conversion in the PA66 laminate composites. As seen from Table V, this profile led to a higher overall crystallinity of the neat APA6 and to an α/γ ratio being almost three times higher than that of the APA6 prepared by isothermal AAROP at 165°C (Table IV). As to the PL laminate composites, the presence of PA66 reinforcements does not imply significant changes in the polymorph content of the matrix of the as-prepared PL samples. The influence of the PA66 reinforcing phase is stronger after recrystallization. The overall crystallinity increases with 10–12% (Table V). Such an effect was not observed with the GFL composites (Table IV). This can be explained by the E-glass fibers being amorphous, whereas the PA66 reinforcements are semicrystalline. Therefore, the PA66 textile would enhance a higher overall crystallinity of the APA6 matrix after recrystallization.

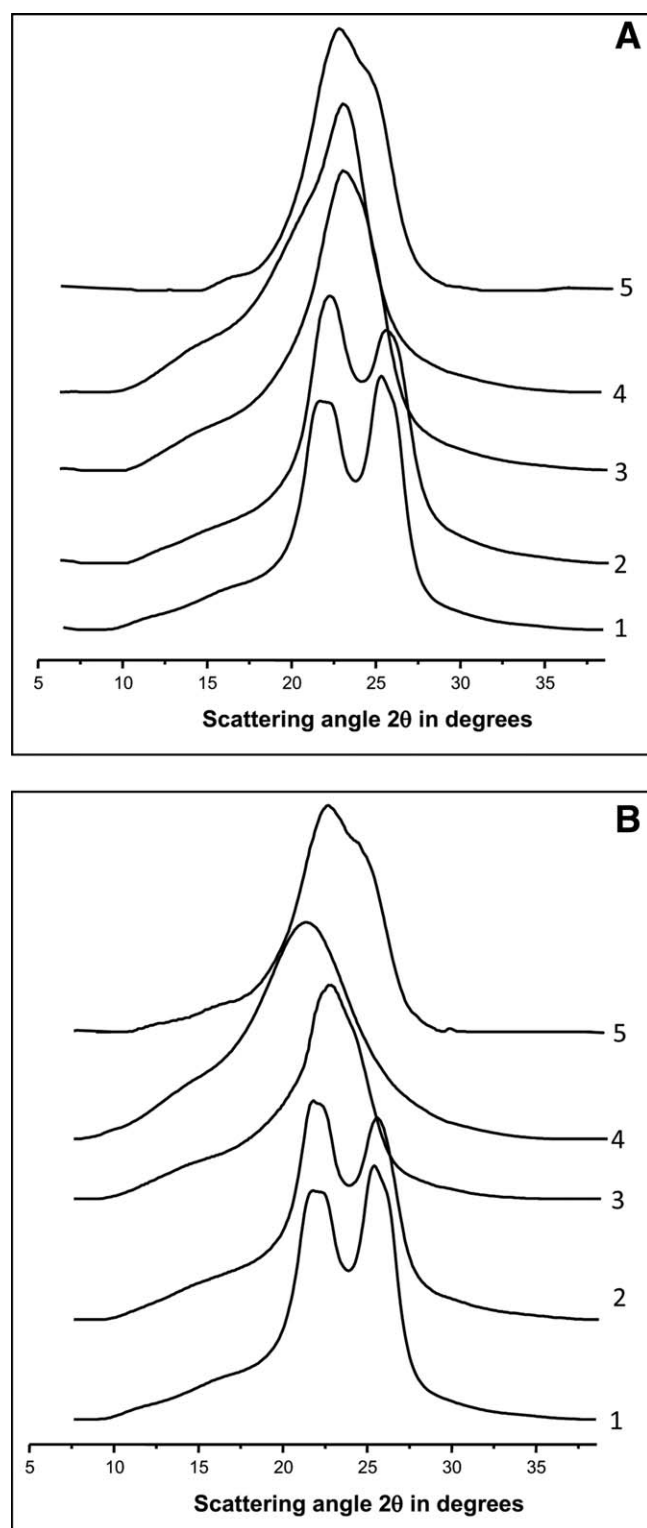


Figure 7. WAXS patterns of APA6/PA66 laminates: (A) no solvent treatment of the PA66 fabrics and (B) with treatment (immersion in acetone). The patterns are obtained at the following temperatures: (2) 30°C; (3) 160°C; (4) 200°C; and (5) 30°C after melting at 260°C. For comparison, the pattern of the neat APA6 at 30°C is displayed in Curve 1.

Table V. Overall Crystallinity and Polymorph Content in Laminate Composites Comprising 10 wt % of PA66 Fabrics with and Without Solvent Treatment When Compared with That of the Respective Neat Matrix

Sample	As Prepared		After Recrystallization	
	Crystallinity (%)	α/γ	Crystallinity (%)	α/γ
APA6	49.9	5.3	52.7	5.3
PL10	48.0	2.1	58.3	0.8
PL10A	48.6	1.2	60.2	1.3

Temperature regime of AAROP was 5 min at 165°C and then gradually cooled to 30°C during 35 min.

CONCLUSIONS

This work proves possible the production of PA6-based laminates reinforced by glass fiber or PA66 textile structures by means of RIM in specially designed prototype equipment. The in-mold AAROP process that creates the matrix reached conversion degrees to PA6 of 97–99% for production cycles of 20 min, which suggests sufficient control over its chemistry and thermal regime. The mechanical strength in tension and impact of the GFL and PL composites produced with volume fractions of reinforcements below 0.25 were with 200–300% higher than the neat matrix material. Light and electron microscopy studies presented evidence for good adhesion at the matrix/reinforcement interface and no void formation during the NYRIM process. According to the X-ray diffraction results, the presence of glass fiber or PA66 fabrics, as well as the temperature conditions of the NYRIM production cycle, can modify the crystalline structure of the PA6 matrix formed by AAROP affecting primarily the α - and γ -polymorph content, especially if additional annealing of the samples is applied.

These findings justify further studies on the NYRIM process so as to evaluate its potential for industrial application. First, the volume fraction of the reinforcements in the laminates should reach 0.5–0.6 without deteriorating the wetting of the textile layers. This would require substitution of the mold with constant thickness integrated into the NYRIM prototype machine by one with variable thickness. Furthermore, comparative mechanical studies and cyclic climate tests involving NYRIM laminates and similar PA6-based composites obtained by conventional processing techniques will be performed. Deeper investigation on the relationship between the matrix crystalline structure and the mechanical performance of the final composite is also needed to optimize the temperature regime and time duration of the NYRIM production cycle.

ACKNOWLEDGMENTS

The authors acknowledge the financial support of HASYLAB at DESY (Grant Number II-07-011EC) and of the Strategic Project LA 25-2011-2012 financed by Fundação para a Ciência e Tecnologia (FCT), Portugal. N. Dencheva is grateful to the FCT for supporting her research by the postdoctoral award SFRH/BPD/45252/2008, cofinanced by QREN-POPH program of the European Union.

REFERENCES

1. Matabola, K. P.; de Vries, A. R.; Moolman, F. S.; Luyt, A. S. *J. Mater. Sci.* **2009**, *44*, 6213.
2. Stavrov, D.; Bersee, H. E. N. *Compos. A: Appl. Sci. Manuf.* **2005**, *36*, 39.
3. Steenkamer, D. A.; Sullivan, J. L. *Compos. B: Eng.* **1988**, *29*, 745.
4. Vaxman, A.; Narkis, M.; Siegmann, A.; Kenig, S. *Polym. Compos.* **1989**, *10*, 449.
5. Schaefer, D. W.; Justice, R. S. *Macromolecules* **2007**, *40*, 8501.
6. Chang, Y. I.; Lees, K. J. *J. Thermoplast. Compos. Mater.* **1988**, *1*, 277.
7. Khondker, O. A.; Ishiaku, U. S.; Nakai, A.; Hamada, H. *J. Polym. Environ.* **2005**, *13*, 115.
8. Svensson, N.; Shishoo, R.; Gilchrist, M. *J. Thermoplast. Compos. Mater.* **1998**, *11*, 22.
9. Bernet, N.; Michaud, V.; Bourban, P.-E.; Manson J.-A. E. *Compos. A: Appl. Sci. Manuf.* **2001**, *32*, 1613.
10. Sakaguchi, M.; Nakai, A.; Hamada, H.; Takeda, N. *Compos. Sci. Technol.* **2000**, *60*, 717.
11. Davé, R. *J. Compos. Mater.* **1990**, *24*, 22.
12. van Rijswijk, K.; Bersee, H. E. N. *Compos. A: Appl. Sci. Manuf.* **2007**, *38*, 666.
13. Gabbert, J. D.; Hedrick, R. M. *Polym. Process. Eng.* **1986**, *4*, 359.
14. Sekiguchi, H. In *Ring Opening Polymerization*; Ivin, K. J.; Saegusa, T., Eds.; Elsevier: New York, **1984**; Vol. 2, p 809.
15. Roda, J. In *Handbook of Ring-Opening Polymerization*; Dubois, P.; Coulembier, O.; Raquez, J.-M., Eds.; Wiley-VCH: Weinheim, **2009**; Chapter 7, p 177.
16. Gong, Y.; Yang, G. *J. Mater. Sci.* **2010**, *45*, 5237.
17. Luisier, A.; Bourban, P.-E.; Manson, J.-A. E. *Compos. A: Appl. Sci. Manuf.* **2003**, *34*, 583.
18. Cho, B. G.; McCarthy, S. P.; Fanucci, J. P.; Nolet, S. C. *Polym. Compos.* **1996**, *17*, 673.
19. van Rijswijk, K.; Bersee, H. E. N.; Jager, W. F.; Picken, S. *J. Compos. A: Appl. Sci. Manuf.* **2005**, *37*, 949.
20. van Rijswijk, K.; Bersee, H. E. N.; Beukers, A.; Picken, S. J.; van Geenen, A. A. *Polym. Test.* **2006**, *25*, 392.
21. Harkin-Jones, E.; Crawford, R. *J. Adv. Polym. Technol.* **1996**, *15*, 71.
22. Harkin-Jones, E.; Crawford, R. *J. Polym. Eng. Sci.* **1996**, *36*, 615.
23. Barhoumi, N.; Maazouz, A.; Jaziri, M.; Abdelhedi, R. *eXPRESS Polym. Lett.* **2013**, *7*, 76.
24. Ryan, A. J.; Stanford, J. L.; Still, R. H. *Polymer* **1991**, *32*, 1426.
25. Nunes, M. I.; Santos, R. J.; Dias, M. M.; Lopes, J. C. B. *Chem. Eng. Sci.* **2012**, *74*, 276.
26. Dencheva, N.; Denchev, Z. *J. Appl. Polym. Sci.* **2013**, *130*, 1228.
27. Dencheva, N.; Denchev, Z.; Pouzada, A. S.; Sampaio, A. S.; Rocha, A. M. *J. Mater. Sci.* **2013**, *48*, 7260.
28. Gürdal, Z.; Hafka, R. T.; Hajela, P. *Design and Optimization of Laminated Composite Materials*; Wiley: New York, **1999**.
29. Dan, F.; Vasiliu-Oprea, C. *Colloid Polym. Sci.* **1998**, *276*, 483.
30. Dencheva, N.; Denchev, Z.; Oliveira, M. J.; Funari, S. S. *J. Appl. Polym. Sci.* **2007**, *103*, 2242.
31. Powell, P. C.; Housz, A. J. I. *Engineering with Polymers*, 2nd ed.; Stanley Thornes Publishers Ltd: Cheltenham, UK, **1998**; p 203.
32. Fornes, T. D.; Paul, D. R. *Polymer* **2003**, *44*, 3945.
33. Dencheva, N.; Nunes, T.; Oliveira, M. J.; Denchev, Z. *Polymer* **2005**, *47*, 887.
34. Samon, J. M.; Schultz, J. M.; Hsiao, B. S. *Polymer* **2000**, *41*, 2169.
35. Lincoln, D. M.; Vaia, R. A.; Krishnamoorti, R. *Macromolecules* **2004**, *37*, 4554.